2nd URSI AT-RASC, Gran Canaria, 28 May – 1 June 2018

An efficient implementation of the periodic method of moments for shielding effectiveness calculations of thin-wire grids

Fabian Happ(1), Heinz-D. Brüns(2), and Frank Gronwald(1)
(1) University of Siegen, Reliability of Technical Systems and Electrical Measurement, 57076 Siegen, Germany, e-mail: Frank.Gronwald@uni-siegen.de
(2) Hamburg University of Technology, Institute of Electromagnetic Theory, 21079 Hamburg, Germany

Abstract

In this contribution the periodic method of moments is applied to calculate the electromagnetic field that is scattered by a periodic thin-wire grid if excited by an electromagnetic plane wave. The formalism is implemented in a professional Method of Moment solver and utilizes both an efficient evaluation formula for necessary summations and appropriate basis and testing functions to connect different periodic cells.

1 Introduction

In the context of Electromagnetic Compatibility (EMC) it is of interest to calculate the electromagnetic field that is scattered by thin-wire grids in order to determine the shielding effectiveness of such periodic planar structures [1]. Among the possible numerical approaches the Method of Moments (MoM) is a suitable one since it allows the accurate modeling of thin-wire structures. In case of periodicity it is then particularly efficient to employ the so-called periodic method of moments (PMoM) where periodic Green's functions are used within the relevant integral equations. An application of the PMoM is rather straightforward if the scatterers within each periodic cell are isolated and not connected to neighboring cells. This circumstance has been used in the study of frequency-selective surfaces, for example [2]. In view of actual wire meshes it has been pointed out that connecting adjacent wires of different cells is not trivial and requires a careful choice of basis functions [3] .
In the following an explicit implementation of the periodic method of moments is introduced which admits connected wire elements across different cells by the choice of special basis functions. This formalism, which has been implemented in a professional MoM software [4], allows the efficient calculation of periodic thin-wire meshes.
The outline of this paper is as follows: In Section 2 the general structure of scattered fields of periodic thin-wire grids is reviewed and put in Section 3 into a MoM formulation. In Section 3 suitable basis and testing functions are introduced as well. Two numerical examples are provided in Section 4 which demonstrate the usefulness of the presented PMoM formulation.

2 Scattered fields of periodic thin-wire grids

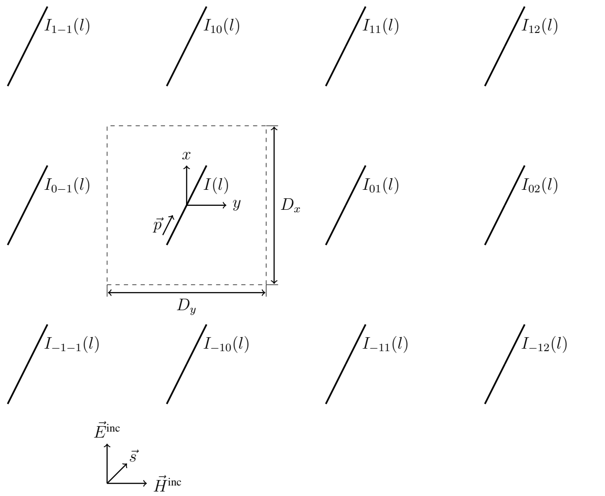

Figure 1. Periodic thin-wire array within the xy-plane. Each unit cell is of dimension D_x and D_y. A unit vector $\vec{p}$ along each wire, a current distriction $I(l)$, and an incident plane wave with unit propagation vector $\vec{s}$ is indicated as well.

The starting point of the following consideration is a periodic arrangement of wires, as shown by an example in Fig. 1. Each unit cell contains one or several wire segments which may be connected or disconnected. The array is located in the xy-plane and excited by an incident plane wave with electric field

$$\vec{E}^{\text{inc}}(\vec{R}) = \vec{E}_0 \exp\left(-j\beta\vec{s}\cdot\vec{R}\right), \tag{1}$$

polarisation vector $\vec{E}_0$, observation point $\vec{R} = (x,y,z)^T$, unit propagation vector $\vec{s} = (s_x, s_y, s_z)^T$, and wave number $\beta = \frac{\omega}{c} = \frac{2\pi}{\lambda}$. Here, c denotes the velocity of light, ω the angular frequency, and λ the wavelength. Utilizing the reference current $I(l)$, all currents can be written in the form

$$I_{qm} = I(l)\exp(-j\beta s_x q D_x)\exp(-j\beta s_y m D_y) \tag{2}$$

with q and m the index of each element in x- and y-direction, respectively. To calculate the electromagnetic field generated by the currents (2) one can follow [5, 2] and first focus on the magnetic vector potential $\vec{A}$ which is generated by (2) if Hertzian dipoles are considered as current elements,

$$d\vec{A}(x,y,z) = \vec{p}\,\frac{dl}{4\pi}\sum_{q=-\infty}^{\infty}\sum_{m=-\infty}^{\infty} I_{qm}\frac{\exp(-j\beta R_{qm})}{R_{qm}}\,, \quad (3)$$

with

$$R_{qm}^2 = (x-qD_x)^2 + (y-mD_y)^2 + z^2\,. \quad (4)$$

For better convergence it is then useful to apply a two-dimensional spatial Fourier transformation which leads to [5]

$$d\vec{A}(x,y,z) = \vec{p}\,\frac{Idl}{2j\beta D_x D_y}\sum_{n_x=-\infty}^{\infty}\sum_{n_y=-\infty}^{\infty}\frac{\exp(-j\beta\vec{R}\cdot\vec{r}_\pm)}{r_z} \quad (5)$$

where

$$\vec{r}_\pm = (r_x, r_y, \pm r_z) \qquad \text{for } z \gtrless 0\,, \quad (6)$$

$$r_x = s_x + \frac{n_x\lambda}{D_x}\,, \quad (7)$$

$$r_y = s_y + \frac{n_y\lambda}{D_y}\,, \quad (8)$$

and

$$r_z = \begin{cases}\sqrt{1-r_x^2-r_y^2} & \text{for } r_x^2+r_y^2<1\\ -j\sqrt{r_x^2+r_y^2-1} & \text{for } r_x^2+r_y^2>1\end{cases}. \quad (9)$$

With $\vec{H} = \vec{\nabla}\times\vec{A}$ and $\vec{E} = \frac{1}{j\omega\varepsilon}\vec{\nabla}\times\vec{H}$ the corresponding electric and magnetic field can be calculated as

$$d\vec{H} = \frac{Idl}{2D_xD_y}\sum_{n_x=-\infty}^{\infty}\sum_{n_y=-\infty}^{\infty}\frac{\exp(-j\beta\vec{R}\cdot\vec{r}_\pm)}{r_z}\,\vec{p}\times\vec{r}_\pm \quad (10)$$

and

$$d\vec{E} = Idl\frac{Z_0}{2D_xD_y}\sum_{n_x=-\infty}^{\infty}\sum_{n_y=-\infty}^{\infty}\frac{\exp(-j\beta\vec{R}\cdot\vec{r}_\pm)}{r_z}\,\vec{e}_\pm \quad (11)$$

with the polarization vector

$$\vec{e}_\pm = (\vec{p}\times\vec{r}_\pm)\times\vec{r}_\pm = (\vec{p}\cdot\vec{r}_\pm)\cdot\vec{r}_\pm - \vec{p} \quad (12)$$

for each mode (n_x, n_y). To calculate the electromagnetic field for an arbitrary current distribution $I(l)$ the expressions above can be integrated, yielding

$$\vec{E} = \frac{Z_0}{2D_xD_y}\sum_{n_x=-\infty}^{\infty}\sum_{n_y=-\infty}^{\infty}\frac{\exp(-j\beta\vec{R}\cdot\vec{r}_\pm)}{r_z}\,\vec{e}_\pm \cdot\int I(l)\exp(j\beta\vec{R}'\cdot\vec{r}_\pm)\,dl' \quad (13)$$

and

$$\vec{H} = \frac{1}{2D_xD_y}\sum_{n_x=-\infty}^{\infty}\sum_{n_y=-\infty}^{\infty}\frac{\exp(-j\beta\vec{R}\cdot\vec{r}_\pm)}{r_z}\,\vec{p}\times\vec{r}_\pm \cdot\int I(l)\exp(j\beta\vec{R}'\cdot\vec{r}_\pm)\,dl'\,. \quad (14)$$

It remains to determine the current $I(l)$.

3 Modelling of periodic thin-wire grids by the method of moments

To numerically obtain the *a priori* unknown current $I(l)$ and by assuming perfect conductivity it is possible to start from the boundary condition

$$\left(\vec{E}(I(l)) + \vec{E}^{\text{inc}}\right)_{\tan} = 0 \quad (15)$$

with $\vec{E}^{\text{inc}}$ defined in (1) and $\vec{E}(I(l))$ given by (13). Introducing test functions $\vec{t}_m$ along the wire surface yields

$$-\int \vec{t}_m\cdot\vec{E}(I(l))dl = \int \vec{t}_m\cdot\vec{E}^{\text{inc}}dl\,. \quad (16)$$

Expanding the current in terms of basis functions f_n with unknown amplitudes I_n according to

$$I(l) \approx \sum_{n=1}^{N} f_n I_n \quad (17)$$

leads to

$$-\sum_{n=1}^{N} I_n\int \vec{t}_m\cdot\vec{E}(f_n)dl = \int \vec{t}_m\cdot\vec{E}^{\text{inc}}dl\,. \quad (18)$$

This implies the linear system of equations

$$\mathbf{Z}\cdot\mathbf{i} = \mathbf{u} \quad (19)$$

where the unknowns I_n constitute the vector $\mathbf{i}$. The matrix $\mathbf{Z}$ has elements

$$Z_{mn} = -\int \vec{t}_m\cdot\vec{E}(f_n)dl \quad (20)$$

and the entries of $\mathbf{u}$ are given by

$$u_m = \int \vec{t}_m\cdot\vec{E}^{\text{inc}}dl\,. \quad (21)$$

The remaining tasks are to define appropriate basis and test functions and to efficiently evaluate the matrix elements Z_{mn}.

In the MoM formulation of the CONCEPT-II software, various sets of basis and test functions are implemented [4]. In the current context it is beneficial to use triangular basis functions f_n and constant test functions $\vec{t}_n$. The constant test functions are defined between the centers of adjacent wire segments and have been introduced in [6], while the linear triangular basis functions are well-known and of the generic form

$$f_n = \begin{cases} p & \text{for a segment } n\\ 1-p & \text{for a segment } n+1\end{cases} \quad (22)$$

with a parameter p. In Fig. 2 these functions are sketched for a straight wire element.

With the choice of constant test functions $\vec{t}_m$ and the expression (13) for the electric field, the matrix elements (20) can

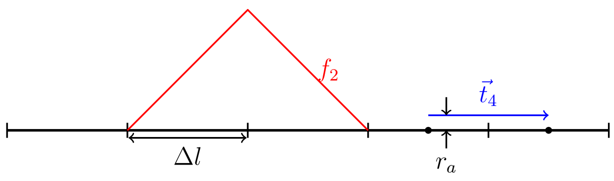

Figure 2. Straight wire element, subdivided into segments of length Δl. Counting from the left, the second triangular basis function f_2 is shown. The fourth test function $\vec{t}_4$ is shown as well. It is defined at the surface of the wire with radius r_a.

explicitly be written as

$$Z_{mn} = -\frac{Z_0}{2D_xD_y}\sum_{n_x=-N_x}^{N_x}\sum_{n_y=-N_y}^{N_y}\frac{\vec{t}_m\cdot\vec{e}_\pm}{r_z} \cdot\int \exp(-j\beta\vec{R}\cdot\vec{r}_\pm)\,dl\int f_n(l')\exp(j\beta\vec{R}'\cdot\vec{r}_\pm)\,dl'. \quad (23)$$

That is, for each combination (n_x, n_y) two integrals need to be evaluated. Fortunately, the integrals can be evaluated analytically since they only contain exponential functions or the product of an exponential function and a linear function. This considerably reduces the effort of explicitly evaluating (23).

More general wire configurations can be treated by the same pattern, that is, by defining triangular basis functions, constant test functions, and an analytical evaluation of the resulting integrals for the calculation of the matrix elements Z_{mn}. Without explicitly going into the details, the following figures indicate appropriate definitions: In Fig. 3 it is shown how to connect different straight wire elements, that are not necessarily in parallel, by overlapping basis functions. To connect wire elements across different cells of a periodic wire array, half-triangular basis functions are introduced, as shown in Fig. 4.

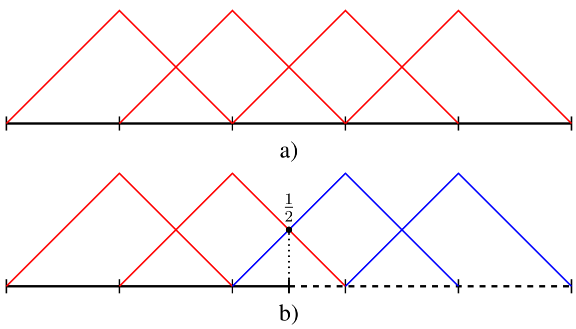

Figure 3. The upper part a) of the figure repeats the usual choice of triangular basis functions for a straight wire element. In the lower part b) of the figure two different wire elements are indicated by a solid and a dashed line, respectively. In contrast to the figure, these wire elements not necessarily need to be in parallel. Now overlapping triangular basis functions of each wire element extend to a neighboring wire element.

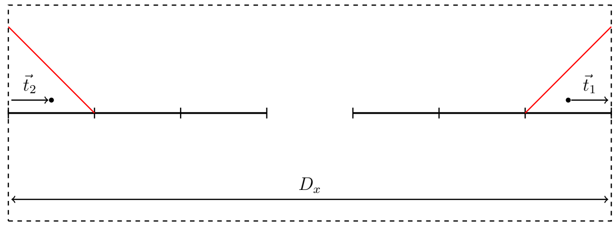

Figure 4. Definition of basis functions and test functions to connect wire elements across different cells of a periodic wire arrangement.

4 Sample calculations and numerical results

The described formulas and procedures have been implemented in the CONCEPT-II software which can be operated by a convenient graphical user interface [4]. Results are illustrated by the following two examples:

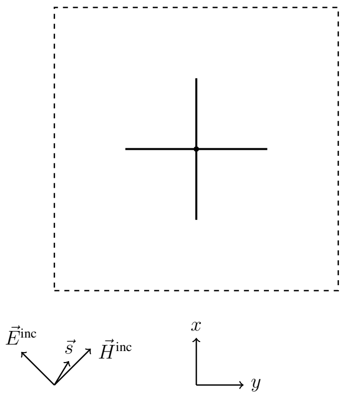

Figure 5. Definition of a unit cell which contains four wire elements that form a symmetric cross.

In Fig. 5 a unit cell is displayed which defines a periodic arrangement of symmetric crosses. This arrangement is excited by a plane wave with $\vec{s} = (0,5;0,5;0,707)^T$ and $\vec{E}_0 = (0,707;-0,707;0)^T$ V/m at a frequency of 1 GHz. The wire radii are $r_a = 1$ mm and each of the four wire elements has length $l = 0,05$ m. As a result, Fig. 6 shows the absolute value of the electric field, calculated at a distance $z = 1$ cm behind the array by both the proposed PMoM and the usual MoM applied to a finite 27×27 array as an approximation of an array of infinite extent. The results obtained by the different methods are in good agreement and validate the PMoM implementation. Of course, the numerical advantages of the PMoM become more and more apparent for electrically small mesh sizes which require a corresponding fine discretisation.

As a second example, Fig. 7 defines a periodic, rectangular wire mesh. A plane wave perpendicularly impinges on the wire mesh with polarization vector $\vec{E}_0 = (0,707;0,707,0)$ V/m. The resulting electric and magnetic fields are evaluated at a distance of 1 cm behind the wire mesh to calculate the frequency dependency of the electric and magnetic shielding effectiveness, as shown in Fig. 7.

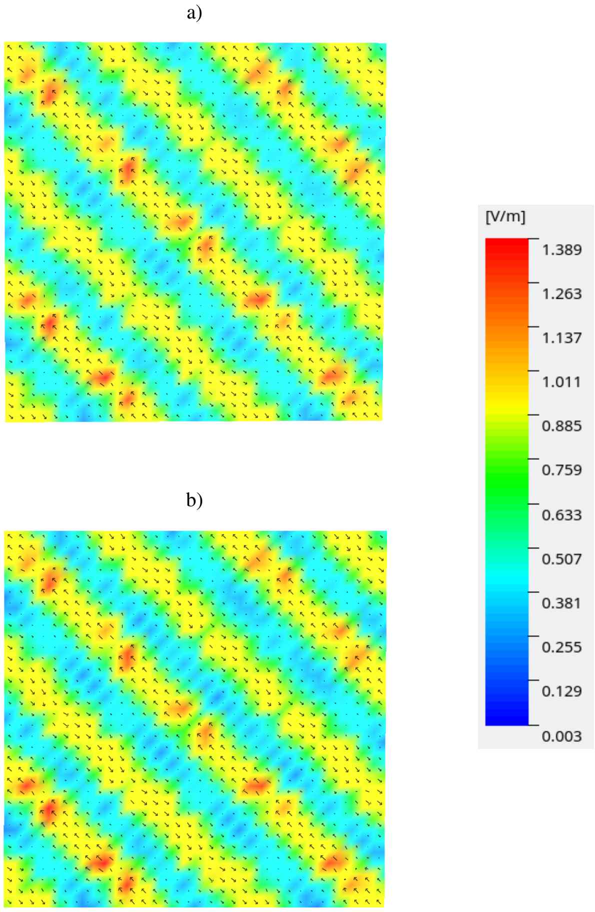

Figure 6. Absolute value of the electric field, calculated at a distance $z = 1$ cm behind the periodic array of symmetric wire crosses.

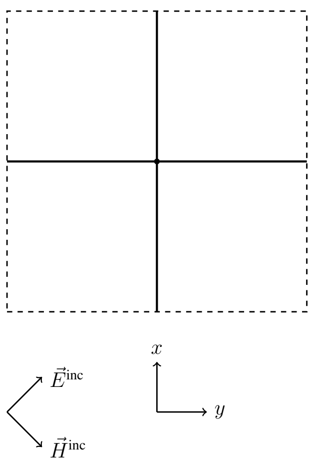

Figure 7. Definition of a unit cell which leads to a periodic wire mesh, excited by a plane wave. The unit cell is quadratic and of dimensions $D_x = D_y = 0.05$ m.

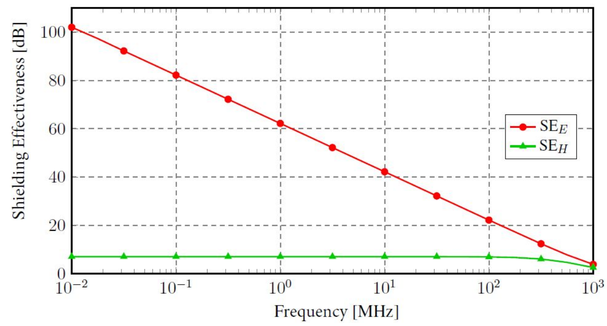

Figure 8. Electric and magnetic shielding effectiveness, calculated for the wire mesh defined by the unit cell of Fig. 7.

5 Acknowledgements

This research was supported in part by the German Research Foundation (Deutsche Forschungsgemeinschaft, DFG).

References

[1] S. Celozzi: *Electromagnetic Shielding*, (Wiley-IEEE Press, New York, 2008).

[2] J. Blackburn and L. R. Arnaut: "Numerical convergence in periodic method of moments analysis of frequency-selective surfaces based on wire elements", *IEEE Transactions on Antennas and Propagation*, vol. 53, (October 2005), pp. 3308–3315.

[3] S.E. Bayer Keskin and A.A. Ergin: "Continuity of currents across neighboring cells in PMM analysis of thin-wire grids", *Turkish Journal of Electrical Engineering & Computer Sciences*, vol. 22, (2014), 582–587.

[4] Technische Universität Hamburg-Harburg. CONCEPT-II. [Online]. Available: http://www.tet.tuhh.de/concept/ .

[5] B. Munk and G. Burrell: "Plane-wave expansion for arrays of arbitrarily oriented piecewise linear elements and its application in determining the impedance of a single linear antenna in a lossy half-space", *IEEE Transactions on Antennas and Propagation*, vol. 27, (May 1979), pp. 331–343.

[6] T. Mader: "Berechnung elektromagnetischer Felderscheinungen in abschnittsweise homogenen Medien mit Oberflächenstromsimulation", (in german) PhD thesis, (Hamburg University of Technology, 1992).